

A VISUAL EXPERIMENTAL TECHNIQUE FOR PLANING CRAFT PERFORMANCE IN CALM WATER AND IN WAVES

by J.I.R.Blake¹ and P.A.Wilson¹(Member)

SUMMARY

The understanding and quantification of hydrodynamic lift requires a full appreciation of the phenomena associated with high-speed planing. Repeatability of results is a major problem with planing craft experiments due to the complexity of fluid flows; wetted lengths, for example, are difficult to measure because of the obscurity created by spray-jets. This difficulty in measurement can produce subjective interpretation. Therefore, reducing hydrodynamic lift using uncertainly defined factors, such as wetted data, can be misleading. This paper outlines an experimental method, Computer Vision Data Acquisition (CVDA), that can remove questions of uncertainty regarding dynamic phenomena by remotely capturing large amounts of planing data for immediate and archival use. An example of the importance of this form of data capture and analysis is described by the ability to validate predictive formulae for planing performance in calm water, and to further advance these formulae for predictions outside their designed realms: in waves.

NOMENCLATURE

A	coefficient used in equation (7)
B	chine beam of planing craft or coefficient used in equation (7)
b	chine beam (used in Section 3.3.1 and)
β	craft deadrise (degrees)
C	coefficient used in equation (7)
C_f	skin friction coefficient
C_{L_0}	lift coefficient for flat plate ($\Delta/0.5\rho V^2 B^2$)
$C_{L\beta}$	lift coefficient for hull with deadrise ($\Delta/0.5\rho V^2 B^2$)
C_{Δ}	load coefficient ($\Delta/\rho g B^3$)
C_v	speed coefficient (V/\sqrt{gB})
CVDA	Computer Vision Data Acquisition
D	depth of hull
Δ	craft weight
EDA	Electronic Data Acquisition
g	acceleration due to gravity
H	waveheight
k	wavenumber ($2\pi/\lambda$)
k_y	radius of gyration
L	craft length overall
LCG	longitudinal centre of gravity (from transom)
L_c	chine wetted length
L_{fe}	craft length overall in feet (used in Taylor Quotient, $V_k/\sqrt{L_{\text{fe}}}$)
L_m	mean wetted length ($0.5(L_c + L_{\text{fe}})$)
L_k	keel wetted length
LWL	static waterline length
λ	wavelength (mean wetted length in)
p	distance from transom to centre of pressure (Figure 8)
$\theta(t)$	pitch angle

θ	pitch magnitude
R	total craft resistance
R_0	calm water resistance
R_n	Reynold's Number
R_w	rough water resistance
R_{AW}	resistance increment in waves ($R_w - R_0$)
ρ	density of water
τ	calm water running trim angle
V	craft forward velocity
VCG	vertical centre of gravity above keel
V_k	craft forward velocity in knots (used in Taylor Quotient, $V_k/\sqrt{L_{\text{fe}}}$)
V_f	average fluid flow velocity on craft bottom
$z(t)$	heave
z	heave magnitude

1. INTRODUCTION.

As high-speed planing craft enjoy increasing popularity in commercial and private use, research into planing craft performance becomes increasingly more important [1]. The accurate theoretical prediction of planing craft performance in calm water and in waves requires complete understanding of the associated phenomena. To this end, experiments need to be conducted and instrumented carefully so that individual components associated with planing can be accurately quantified – providing validation of numerical codes and highlighting areas for further research.

Experimental work has been undertaken by many (extensively cited by Payne, [2] to [10]) to identify the various components of lift and the effect of hull geometry parameters and speed. Much of the previous theoretical and experimental work on planing has been centred on calm water performance (examples include Sottori [11]; Shoemaker [12]; Sambras [13]; Korvin-Kroukovsky *et al* [14]; Savitsky and Neidinger [15]; Savitsky [16]), with

¹ Fluid Structure Integration Research Group, University of Southampton

comparatively little experimental and theoretical investigation into performance in waves.

Identification of lift components requires understanding of the flow phenomena associated with the hull. The dynamic lift of a planing hull is dependent, among other factors, on wetted surface but the influence of this variable on lift is difficult to isolate because of the problem of accurate wetted surface measurement.

Payne [10] summarises the problems that experimenters have had in relating the lift force to individual parameters, especially in terms of wetted lengths, and describes the degree of variation in over 1000 experimental results. A wide range of formulae exist that attempt to predict the total lift on planing surfaces, but due to the amount of scatter between individual experimental results, most theories have general exceptions as to their applicability, Figure 1. Reducing the variation of experimental planing data would reduce the chances of misinterpreting the importance of specific planing phenomena – improving the empiricisms that ensue and allowing more generalised theories. These problems abound for planing craft performance in calm water; the problem of identification of specific qualities is even more complicated by the craft's operation in a seaway.

An experimental method is required that can accurately measure wetted surface data. With this in mind, the experimental investigation described herein was initiated. The purpose of the investigation was to test a largely unused technique (Computer Vision Data Acquisition, CVDA) to measure specific quantities, such as wetted surface, in a consistent manner which is repeatable from test to test, in this way enabling the degree of scatter discussed above to be reduced.

Using an existing set of experimental data [17][18], the results obtained from the authors' recent tests could be compared – highlighting the possible problems with test repeatability and providing an ability to compare each set of experimental results with standard planing performance equations [16].

Finally, the extraction of data fundamental to planing craft performance (i.e. wetted surface data) in calm water is shown to have important bearing on the ability to predict performance in waves.

1.1. Computer Vision Data Acquisition

For craft moving in waves, the quantification of relative motions between a point on the hull surface and the water provides useful data and appreciation of experienced accelerations. Wetted data also provides resistance information both in calm water and in waves. Typically these quantities have been extracted from experimental tests by the use of resistance or capacitance probes.

For craft travelling at high speed, the amount of generated spray reduces the ability of resistance and capacitance probes to accurately quantify wetted length and surface values. Techniques to avoid this problem and to investigate underwater surface flows have involved the use of still photographs [16][19], and limited video analysis [17].

More than just those aforementioned physical effects can be analysed by video. In fact, all displacements, velocities and accelerations can also be measured. The benefits of accurately acquiring information by video are enormous. Conventionally, large amounts of instrumentation and equipment are required to acquire all the necessary data from tank testing. This results in added weight to the model, more calibration and the increased possibility of noisy cross-talk in multiplexed signals. The use of video avoids these problems by capturing all the data at once without any interference with the model and the effects it is trying to measure. Video capture also has no influence on the objects

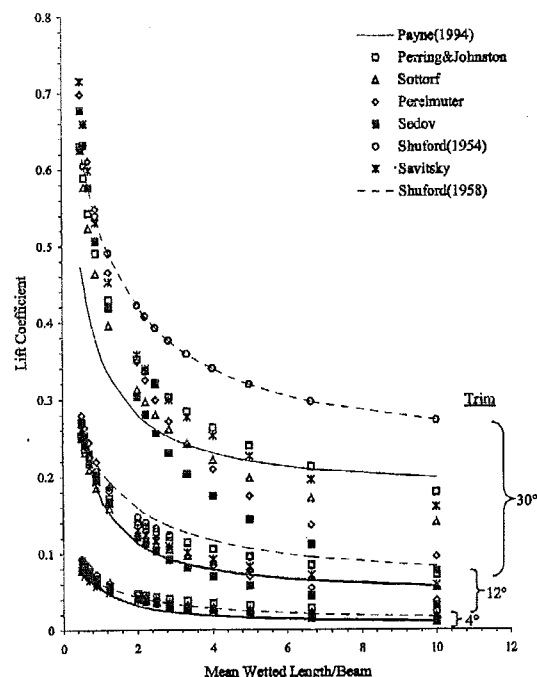


Figure 1 Comparison of various theories for flat plate lift. Lift coefficient based upon aspect ratio (B/L_m).

in question since there is no added damping due to moving mechanisms that would ordinarily be monitoring displacement, velocities and accelerations; these can all be measured remotely. The system is self-calibrating since all the calibration information is contained within each frame of information.

The equipment required for this particular data acquisition technique is reduced to a power source, high definition video cameras and a powerful computer. To this end a computer vision system is employed whereby the visual data is acquired, converted to digital form and digitally analysed. Once the data has been recorded, it can be reviewed at any time with the ability to focus on any particular phenomenon desired. Provided the video analysis hardware and software are capable enough, video footage of any object moving in any environment could be analysed. This information can be archived, then analysed and critically re-evaluated at any point.

The restriction on this type of data acquisition is at present large since the hardware and software required for accurate automatic identification of points of interest – specific locations within the frame for which coordinate information is required – from frame to frame is expensive. The final extraction of the points of interest were carried out manually. So although one of the main advantages is the amount of information that can be captured simultaneously, the actual amount of information that can be processed at present is limited to a few frames, equivalent to a couple of seconds of data.

2. EXPERIMENTAL PROGRAMME

Fridsma conducted a parametric series of tests to analyse the performance of constant deadrise planing hulls in calm water, regular [17] and irregular seas [18]. This extensive and well-referenced experimental programme provided a wealth of information concerning the important parameters associated with planing craft performance.

One craft configuration, Configuration K, based upon the same lines as Fridsma's constant deadrise monohulls was constructed and tested by the authors. A body plan for Configuration K is given in Figure 2. Fridsma's original model was 1.143m in length overall compared to the authors' craft length of 1.25m. All the

other dimensions and parameters have therefore been appropriately scaled, Table 1.

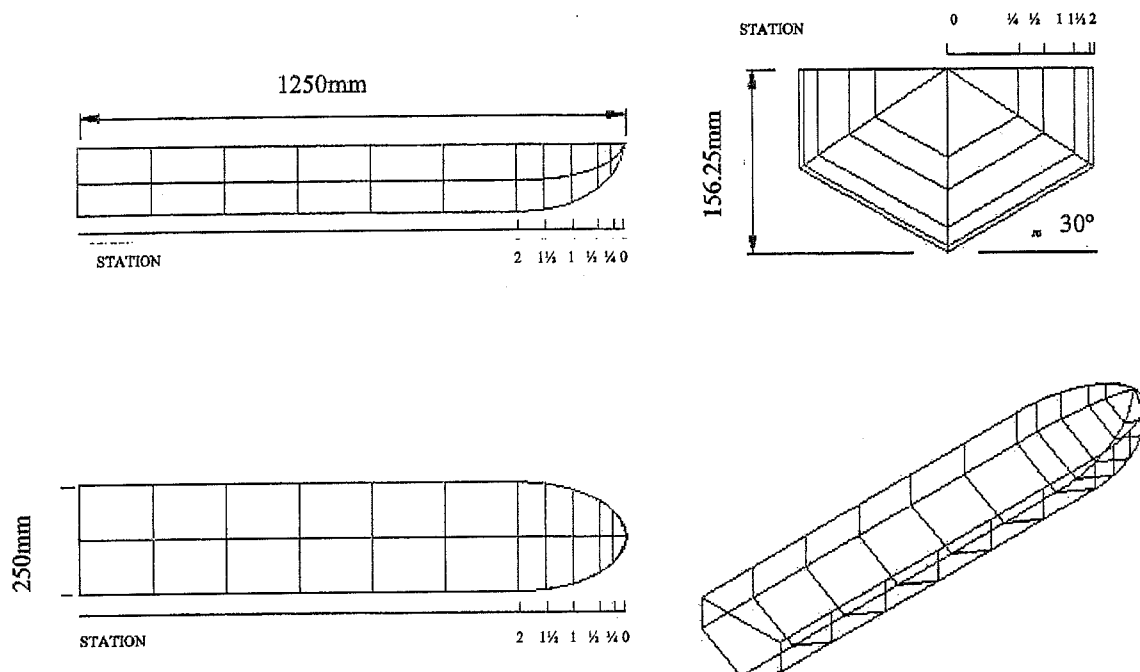


Figure 2 Model lines for Configuration K

LOA, L	1.25m
Static LWL	1.20m
Static Trim	1.4°
Chine Beam, B	0.25m
Depth, D	0.15625m
Deadrise, β	30°
Craft Weight, Δ	93.2N
$C_v (V_k/L_k)$	2.66 (4.00)
L/B	5
B/D	1.6
k/B	1.235
LCG/B (from bow)	1.95
C_A	0.608
VCG/B (above keel)	0.30

Table 1 Experimental Model Particulars (equivalent to Fridsma's Configuration K)

The testing facility used was the towing tank at Southampton Institute, which has a maximum carriage tow speed of 4.2ms⁻¹. Scaling problems restrict the size of the model to at least 1.25m – any smaller and the scaled weight for model length is difficult to achieve.

The ballast was arranged within the model to achieve the correct gyradius, k_v , and zero-speed trim and transom submergence. As in Fridsma's tests, the craft was towed at the centre of gravity and the thrust line was considered to be horizontal and acting through the CG. The craft was allowed

freedom to roll, pitch and heave in order that, through the measurement of sideforce, the model's longitudinal alignment could be checked until there were no asymmetric motions.

Following Fridsma[17] the effect of surge was neglected and the tests were carried out at constant speed. Craft heave and pitch motions were measured in the standard way with translational and rotational transducers. Resistance was measured directly from the dynamometer.

Wave elevation was measured approximately one metre abeam of the CG using a wave probe. It was found from repeated runs with different wave probe locations that this position of the wave probe had no effect on the craft response and that due to the high forward speed the wave patterns from each body did not interfere.

Table 2

H/B	0.111
λ/L	1, 1.5, 2, 3, 4, 6

Table 2 Regular wave test parameters

The tests in waves were carried out in regular head seas of constant waveheight for varying encounter frequency. All data was acquired and output using the WUMTIA (Wolfson Unit of Marine Technology and Industrial Aerodynamics) data acquisition software suite. This standard data acquisition method is referred to henceforth in this paper as Electronic Data Acquisition (EDA).

A grid was defined on one side of the model in 8cm by 1cm patches and below the chine in 1cm by 1cm patches. These patches provide the calibration for the computer vision data acquisition and aid location of particular points of interest. A black and white self-illuminating underwater camera was mounted just above the waterline normal to the direction of tow and opposite the centre of gravity. The camera is connected to a standard VHS video recorder and a monitor. The lighting was positioned to be on-axis to alleviate and minimise shadows.

The trigger point for the Electronic Data Acquisition, EDA, was automatic and data was acquired over 15m, equating to around 3 seconds for a tow speed of 4.2ms^{-1} . Unfortunately the length of acquisition time could not be increased due to the limiting length of the towing tank. Whilst this is not a problem for calm water performance, the number of motion cycles recorded for the tests in waves is restricted, affecting the time-average. This problem may be significant for waves of lower encounter frequency, for example in waves six times the craft length (the lowest tested encounter frequency), the data acquisition will only record around 3 motion cycles. Nevertheless, in terms of comparing the CVDA approach with the EDA approach, the limited acquisition time was not considered important. Furthermore, Fridsma's results described the resonant response for this particular craft configuration to be in wavelengths between three and four boat lengths, which allowed for almost double the number of motion cycles to be recorded compared to the lowest wave encounter frequency.

The computer vision data acquisition was triggered manually after the electronic acquisition had started and stopped before the electronic acquisition stopped. This enabled the video capture of purely steady-state planing and not the capture of information as the craft decelerated at the end of its run.

The VHS information was then digitised using standard Silicon Graphics Media Recorder and Converter software and decomposed into individual JPEG-compressed frames so that 25 frames corresponded to 1 second of real-time data. The intention was to analyse each frame automatically with image recognition hardware and software for significant points of interest. However the limitations, expense and availability of this technology at the time these experiments were conducted in 1997 meant that each frame was manually analysed instead using the image editor XV-3.10a. As technology has improved in Computer Vision systems since the time these experiments were performed (for example in the analysis of human movement), the original video footage could be re-examined but for the purposes of the investigation at the time, manual extraction of points of interest was acceptable.

Co-ordinate information from each digitised frame was taken regarding the deck profile, carriage rail profile, keel/water intersection point and spray sheet/chine intersection. The calibration was taken from the known grid size on the model hull, and the camera orientation from the carriage rail profile. The problem of parallax was readily checked for by looking at the variation of calibration constants over different locations within the captured frames and was found to be negligible. The co-ordinate data was then converted into real quantities and output in the form of heave and pitch displacements and wetted length data.

An example sequence is shown in Figure 4. This sequence is for an experimental run into waves twice the boat length. Two points of interest have been highlighted on the deck edge and the outline of the spray area overlaid onto each image. With small scale models, surface tension effects may present a problem concerning the ability of the fluid flow to detach from the chine. Fridsma attached celluloid strips to the chine-line to force detachment of the spray sheet. The authors' model was only 10% longer than Fridsma's craft, yet it was observed during the tests, and indicated in the white-outlined zone in

Figure 4, that the spray sheet detaches cleanly from the chine. Surface tension effects were, therefore, neglected.

Calm water tests were carried out initially before towing the craft into regular head waves ranging in wavelength from 1 to 6 boat lengths. The calm water tests provide a level of confidence in the CVDA system albeit that the phenomena being recorded are quasi static.

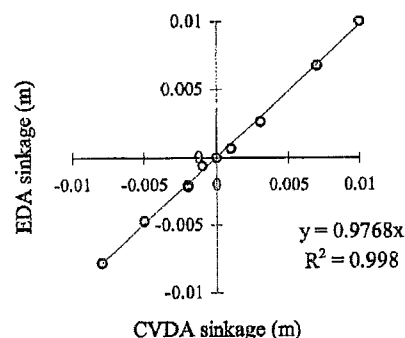


Figure 3 Correlation between CVDA and EDA for measured craft sinkage

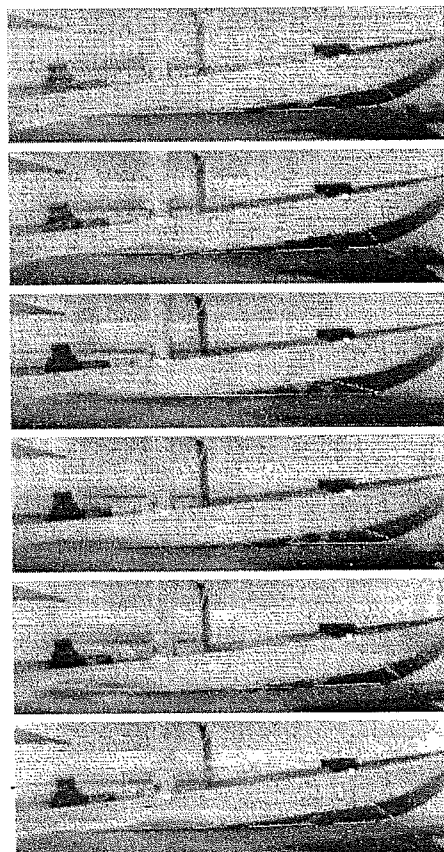


Figure 4 Sequence of digitized images taken every 0.2 seconds. $\lambda/L=2$.

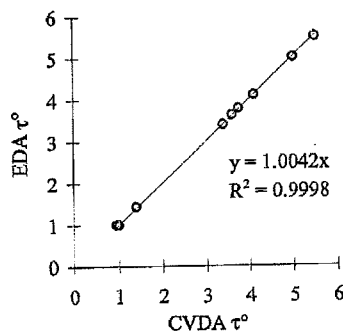


Figure 5 Correlation between CVDA and EDA for measured craft trim

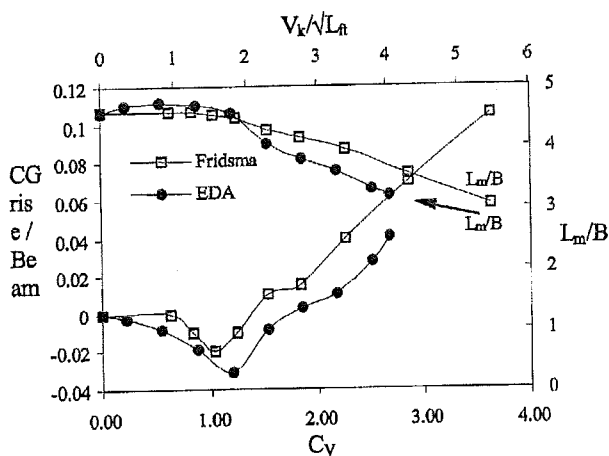


Figure 6 EDA values vs. Fridsma [17] values for craft sinkage. Mean wetted length ratio, L_m/B , evaluated using CVDA.

3. RESULTS

Figure 3 and Figure 5 respectively show the sinkage and trim of the craft from zero to full speed measured using EDA and plotted against the results from the CVDA.

As expected, there is negligible difference between the two systems. Figure 6 and Figure 7 respectively describe the difference in these newly measured (EDA) sinkage and trim values with Fridsma's results. The results are comparable in behaviour although it appears that the new model requires a higher speed for the centre of gravity to rise. The new model sits lower in the water at full planing speed than Fridsma's with a much higher trim angle.

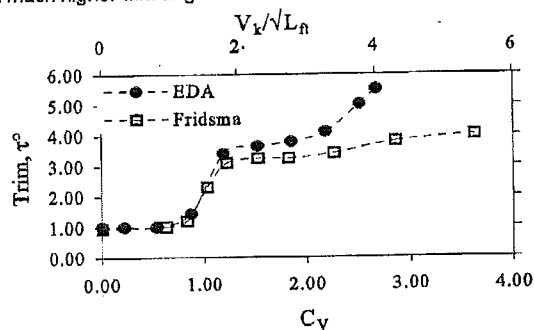


Figure 7 EDA values versus Fridsma [17] values for craft Trim

Wetted length data is measured from the computer vision data acquisition for the range of speeds from zero to a planing speed of $C_v = 2.66$. Comparison with Fridsma's result is good, applicability) Figure 6, but does show a slight decrease in magnitude over the higher speed range ($C_v > 1.00$). This is directly attributable to the increased trim angle for this speed range despite the lower position of the CG in the water.

Sinkage and trim of this particular planing craft configuration can also be determined theoretically. Savitsky [16] includes Koebel *et al*'s [20] plot which summarises the relationship

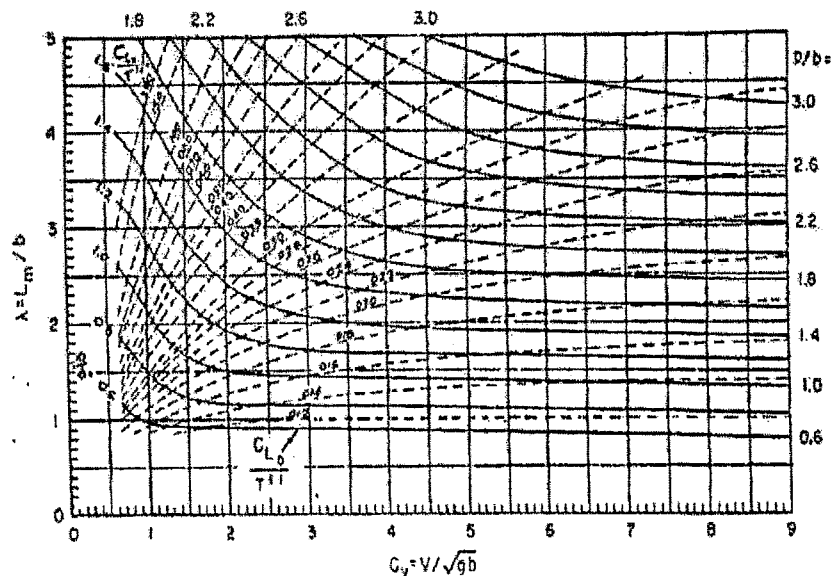


Figure 8 Normogram for equilibrium conditions when all forces act through CG [16][20]

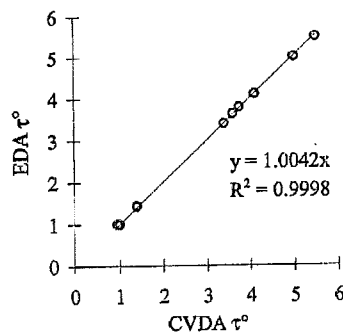


Figure 5 Correlation between CVDA and EDA for measured craft trim

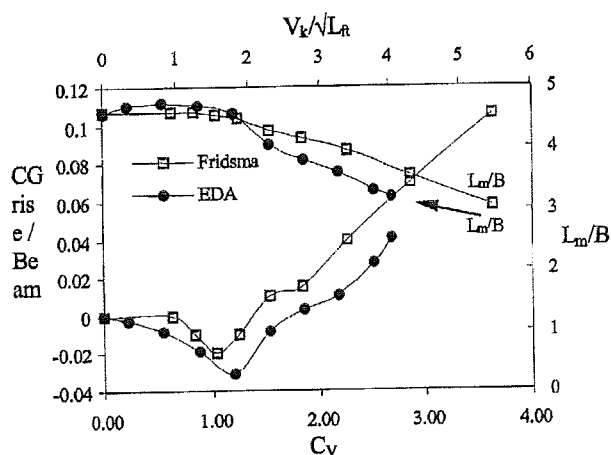


Figure 6 EDA values vs. Fridsma [17] values for craft sinkage. Mean wetted length ratio, L_m/B , evaluated using CVDA.

3. RESULTS

Figure 3 and Figure 5 respectively show the sinkage and trim of the craft from zero to full speed measured using EDA and plotted against the results from the CVDA.

As expected, there is negligible difference between the two systems. Figure 6 and Figure 7 respectively describe the difference in these newly measured (EDA) sinkage and trim values with Fridsma's results. The results are comparable in behaviour although it appears that the new model requires a higher speed for the centre of gravity to rise. The new model sits lower in the water at full planing speed than Fridsma's with a much higher trim angle.

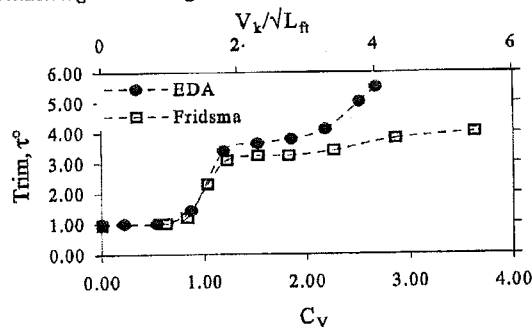


Figure 7 EDA values versus Fridsma [17] values for craft Trim

Wetted length data is measured from the computer vision data acquisition for the range of speeds from zero to a planing speed of $C_v = 2.66$. Comparison with Fridsma's result is good, applicability) Figure 6, but does show a slight decrease in magnitude over the higher speed range ($C_v > 1.00$). This is directly attributable to the increased trim angle for this speed range despite the lower position of the CG in the water.

Sinkage and trim of this particular planing craft configuration can also be determined theoretically. Savitsky [16] includes Koebel *et al*'s [20] plot which summarises the relationship

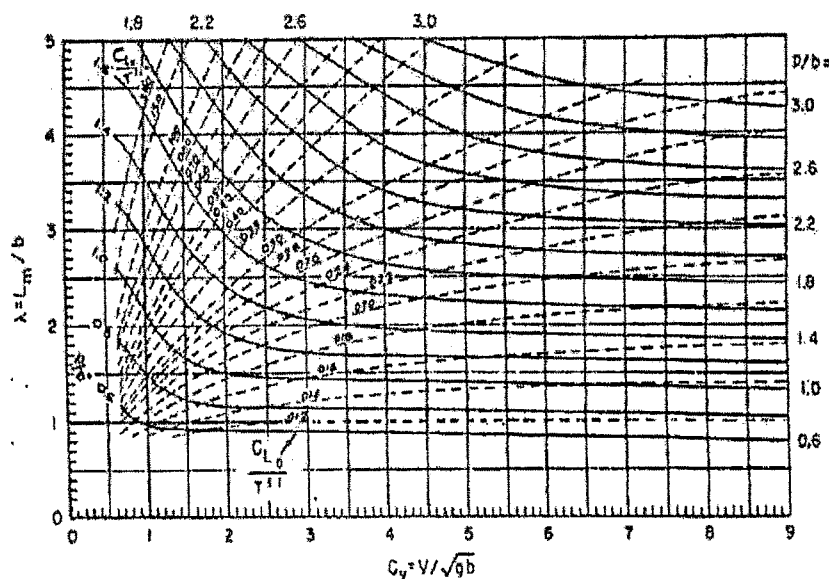


Figure 8 Nomogram for equilibrium conditions when all forces act through CG [16][20]

between planing lift, centre of pressure and wetted area according to Savitsky's equations and making the assumption that all forces act through the centre of gravity. This plot is reproduced in Figure 8.

The validity of the plot is restricted to $2 \leq C_v \leq 13.0$ and $2^\circ \leq \tau \leq 15^\circ$ and $L_m/B \leq 4$. The values of trim and mean wetted length for Fridsma's last three craft speeds (within the range of applicability) are shown in Figure 9 and Figure 10 respectively, and are compared to the authors' experimental values for trim and mean wetted length which fall within the prescribed boundary conditions. The predicted values from Koebel *et al*'s nomogram are represented in the figures by solid lines. These values are derived from knowledge of the distance of the centre of pressure from the transom (the normal force acting through the centre of gravity, $1.95B$ from the transom) and the speed coefficient, C_v .

Whilst the mean wetted length is in good agreement (less than 6% error), the trim angle is generally overpredicted, reducing in error at the highest speed ratio. There are two possible reasons for this. Firstly the lift, a summation of hydrostatic and hydrodynamic components, is underpredicted, requiring a greater immersion to realise a larger hydrostatic contribution to lift. Alternatively, neither the viscous component of drag or the centre of pressure pass through the centre of gravity, thereby negating the applicability of the theory illustrated in Figure 8.

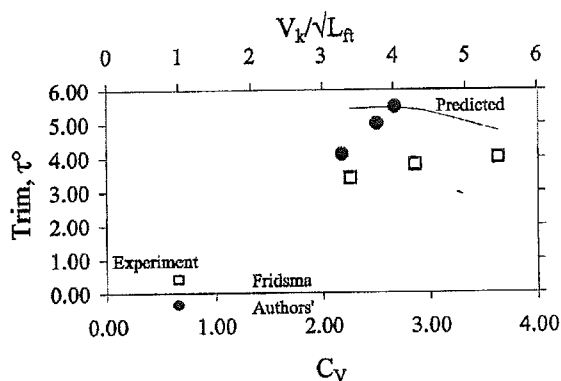


Figure 9 Comparison of experimental and predicted [16] trim values

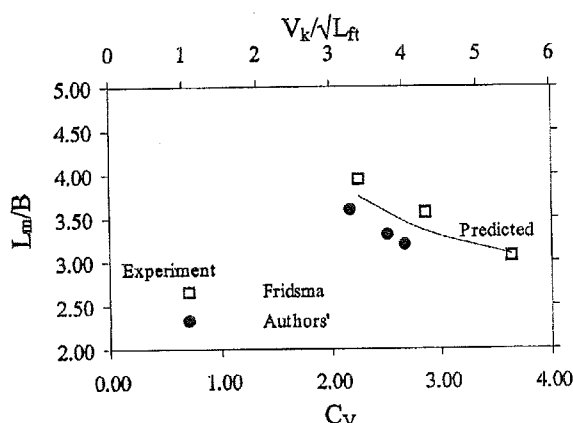


Figure 10 Comparison of experimental and predicted [16] mean wetted length values

The resistance results are shown in Figure 11, and demonstrate that the authors' results compare favourably with Fridsma's results albeit with a higher resistance at larger speed coefficient, $C_v > 1.75$. This is accounted for by the model sitting lower in the water than Fridsma's at full planing speed and with a higher trim angle, adversely affecting both the lift vector angle (increasing the pressure drag) and the viscous component of drag. Figure 12 shows the comparison between the authors' and Fridsma's experimental values of drag/lift ratio and the values of drag/lift from Savitsky's predicted mean wetted length and trim (from Koebel *et al*'s nomogram).

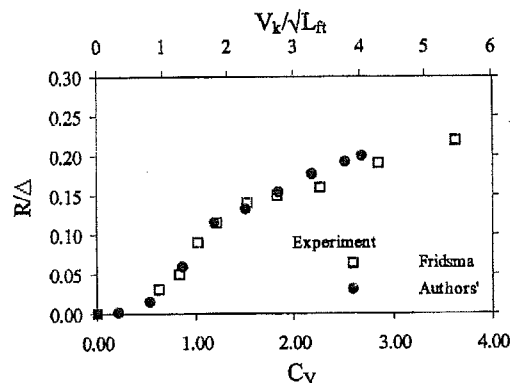


Figure 11 Comparison between Fridsma and authors' experimental values for craft drag/lift ratio

One more plot can also be shown on the same figure, derived from Savitsky's theoretical drag/lift ratio given the experimental values for trim and mean wetted length. From [16], the expression for drag/lift ratio in calm water is given as,

$$\frac{R}{\Delta} = \tan \tau + \frac{C_f \left(\frac{L_m}{B} \right) \left(\frac{V_1}{V} \right)^2}{C_{L\beta} \cos \tau \cos \beta} \quad (1)$$

where V_1/V describes the ratio of the average bottom velocity to the forward planing velocity (see [16] for a full description). The skin friction coefficient, C_f , is defined by the ITTC formula,

$$C_f = \frac{0.075}{[(\log Rn) - 2]^2} \quad (2)$$

The lift coefficient, $C_{L\beta}$, is given by,

$$C_{L\beta} = C_{L0} - 0.0065 \beta C_{L0}^{0.6} \quad (3)$$

where,

$$C_{L0} = \tau^{1.1} \left(0.012 \sqrt{\frac{L_m}{B}} C_v^2 + 0.0055 \left(\frac{L_m}{B} \right)^{\frac{5}{2}} \right) \quad (4)$$

Figure 12 shows that the prediction of drag/lift ratio from experimental mean wetted length and trim is in good agreement with the experiments.

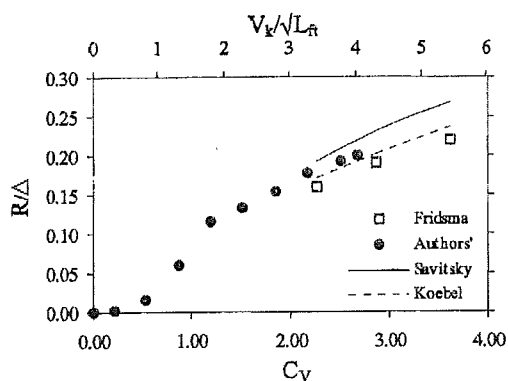


Figure 12 Comparison of experimental and predicted [16] drag/lift ratios

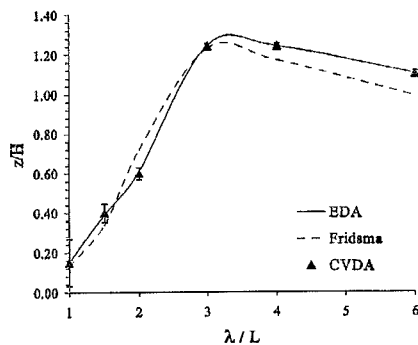


Figure 13 Comparison between Fridsma and authors' experimental values for craft heave (EDA and CVDA)

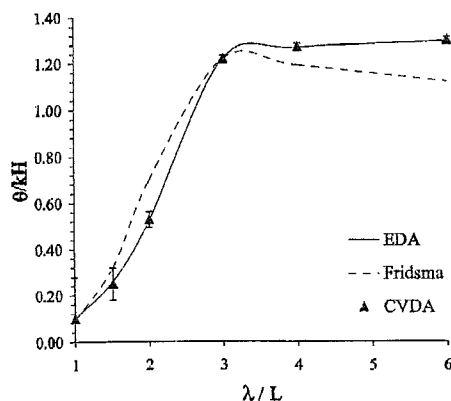


Figure 14 Comparison between Fridsma and authors' experimental values for craft pitch (EDA and CVDA)

3.1. Regular Waves

Figure 13 and Figure 14 show the heave and pitch responses of the craft in regular waves ranging from wavelengths of 1 to 6 craft lengths. The solid lines relate to the measured response through the standard electronic data acquisition, EDA, whilst the triangles correspond to the CVDA approach. Both results are derived from the average magnitude of the peak-peak motions acquired by each respective method. The heave response is non-dimensionalised by waveheight and the pitch response by waveslope.

The results shown are for one particular experimental set which is used as a benchmark - in this manner the CVDA time-histories can be compared directly to the standard electronic data acquisition results, which would be impossible if an average result measured from all the experimental test runs was used.

The magnitude of the peak responses and the frequencies at which they occur agree very well with Fridsma's results for both the EDA and CVDA approaches. However, at longer wavelengths, the boat responses are greater especially for pitch. The calm water discrepancies in running trim and sinkage are undoubtedly a contributory factor, but also the length of time over which the data is acquired will affect the time-average. The test results from the EDA showed little variation between experiments at the higher encounter frequencies but at the longer wavelengths more disparity was evident. This indeed reflects the disadvantage of the restricted data acquisition time.

In order for the whole craft length to be investigated using the CVDA technique, the image can only be calibrated to 1mm. Allowing for a 1mm error in identifying the correct location of a specific point of interest from the CVDA data produces the error bars in the above figures. Since motions of the planing craft move from a platforming condition in short wavelengths to contouring in long wavelengths with increasingly larger excursions about the mean position, the importance of the calibration size and error on the resulting value for peak to peak motion diminishes (from around 20% to 3%). Directing the CVDA on specific areas of interest can circumvent this problem.

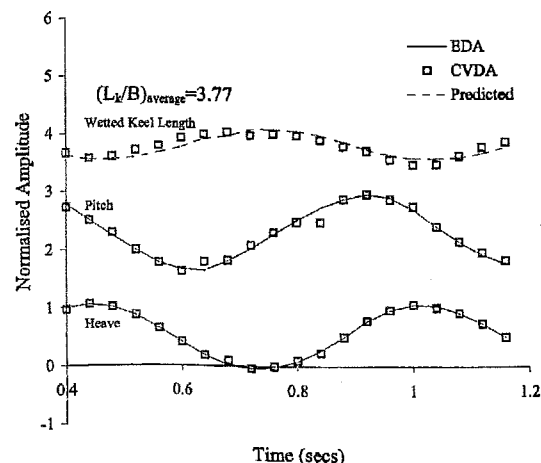


Figure 15 Comparison between time histories of craft motions measured using EDA and CVDA. Wetted length acquired by CVDA vs. predicted values. ($\lambda/L=3$)

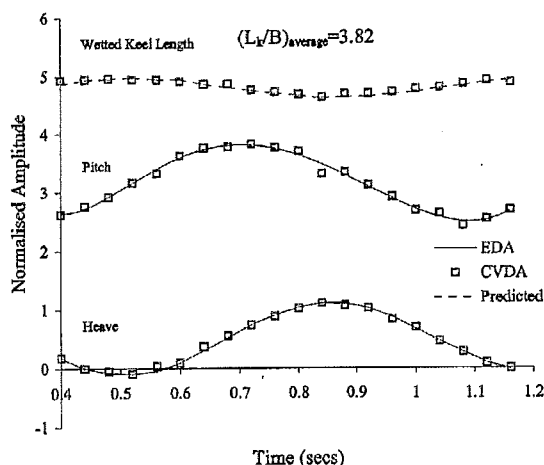


Figure 16 Comparison between time histories of craft motions measured using EDA and CVDA. Wetted length acquired by CVDA vs. predicted values. ($\lambda/L=4$)²

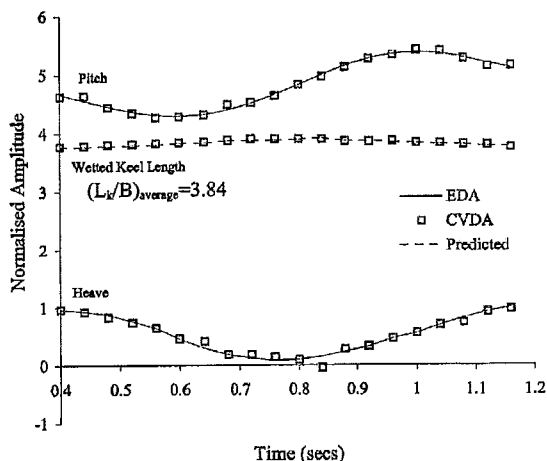


Figure 17 Comparison between time histories of craft motions measured using EDA and CVDA. Wetted length acquired by CVDA vs. predicted values. ($\lambda/L=6$)

A window of the time histories for heave response (normalised with respect to waveheight) and pitch response (normalised with respect to waveslope) is shown in Figure 15 to Figure 17. Wetted keel lengths, normalised with respect to chine beam, are also shown and discussed in Section 3.3. The solid lines refer to the EDA approach whilst the symbols refer to the CVDA results. Error bars are not shown for clarity but heave can be acquired through CVDA to ± 1 mm and pitch to $\pm 0.1^\circ$ for the camera setup described. These time-histories show the correct frequency and, for that part of the run recorded, very similar magnitude in response to the corresponding time history from the EDA.

3.2. Added Resistance

Figure 19 shows the mean rough water resistance of the craft over decreasing encounter frequencies. At longer wavelengths, the craft resistance approaches the calm water value shown in Figure 18. However, as with the calm water

resistance, the resistance in waves is larger than Fridsma's results.

The resistance increment², R_{Aw} , or added resistance when the craft is travelling in waves is shown in Figure 20. This describes the reduction in added resistance with decreasing encounter frequency and in fact at the longer wavelengths, the resistance drops below the calm water value.

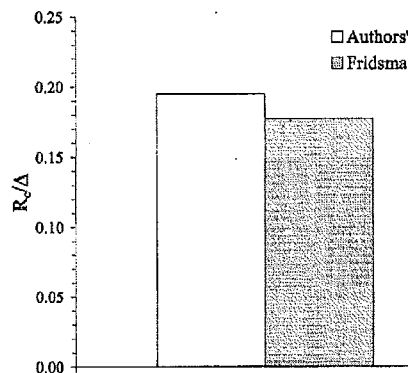


Figure 18 Comparison between Fridsma and authors' experimental values for craft calm water resistance.

3.3. Wetted Data

Wetted keel length data, measured using the CVDA, is shown in Figure 15 to Figure 17, normalised with respect to craft chine beam. Due to time constraints, chine wetted lengths were not recorded. The maximum wetted values occur when heave is a minimum; the pitch angle attenuates the size of the wetted length change. The mean wetted keel length increases slightly with decreasing encounter frequency. The implication of this alone would seem to be that the resistance in waves increases slightly with decreasing encounter frequency – this is not borne

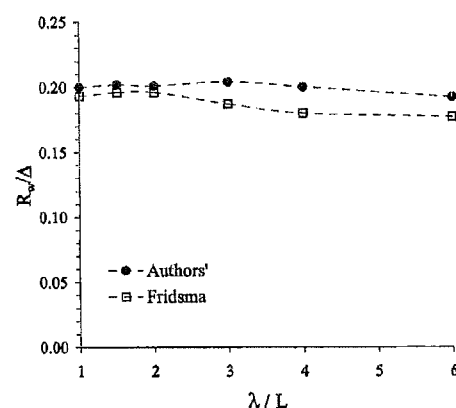


Figure 19 Comparison between Fridsma and authors' experimental values for craft resistance in regular head seas.

² 1.0 has been added to wetted keel length values in Figure 16 for clarity

³ The added resistance is the difference between R_w and R_c

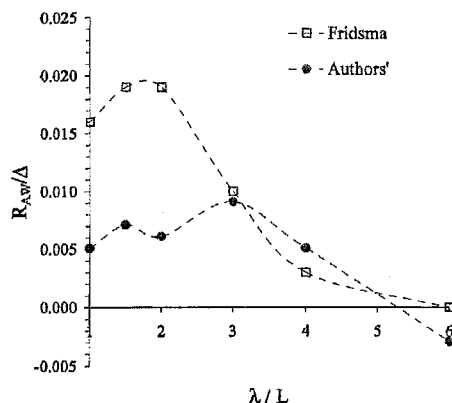


Figure 20 Comparison between Fridsma and authors' experimental values for craft added resistance in waves ($R_w - R_0$).

out by Figure 19 and Figure 20. However, resistance for planing craft is not a function of wetted keel length but a function of mean wetted length. At longer wavelengths, the mean wetted length (an average of the chine and keel wetted lengths) will approach the calm water running value. This requires a slight reduction in the mean wetted chine length to complement the slight increase in mean wetted keel length.

As the magnitude of the wetted surface approaches the calm water running value, the resistance would be expected to as well. However it has already been seen that the resistance at longer encountered wavelengths reduces the resistance below the calm water value. Consequently, for a slightly increasing wetted keel length, the wetted chine length must reduce fairly significantly for the resistance to be less in long waves than in calm water.

This discussion of wetted lengths demonstrates the importance they play in the resistance and lift of the planing craft. A method for predicting these two quantities based upon the wetted lengths would be advantageous which requires the prediction of the wetted lengths in the first instance. In calm water, Savitsky's expressions for wetted lengths based upon trim angle, beam and deadrise show favourable comparison with previous experimental results and, in a limited fashion, the experiments described herein reinforce this confidence. From these expressions, Savitsky relates the subsequently generated lift and resistance which also compare well with experimental results [16]. If these expressions for wetted lengths could be applied dynamically for use in waves then lift and resistance in waves could be predicted.

3.3.1. Wetted Keel Length

Savitsky's expression for wetted keel length in calm water planing is given as

$$L_k = L_m + \frac{b \tan \beta}{2\pi \tan \tau} \quad (5)$$

where τ is the steady-state trim angle, L_m is the mean wetted length, b is the chine beam.

L_k is not a function of time, but if it were then a dynamic equation could be hypothesised as,

$$L_k(t) = L_m(t) + \frac{b \tan \beta}{2\pi \tan \theta(t)} \quad (6)$$

where $\theta(t)$ is the instantaneous pitch angle and is a function of time. Since chine wetted lengths have not been measured in the rough water tests, $L_m(t)$ is replaced by a constant of 3.75 craft beams, an average mean wetted length value from Figure 10 for this craft speed ($C_F=2.66$). Heave is introduced into the equation and coefficients are fitted so that the resulting expression matches measured results. This leads to the following equation,

$$L_k(t) = A \left\{ B + \left(3.75 + \frac{b \tan \beta}{2\pi \tan \theta(t)} \right) - Bz(t) \right\} + C \quad (7)$$

where $z(t)$ is the instantaneous heave, A , B and C are fitted coefficients.

This equation is not explicit, has no rigorous mathematical basis and merely represents curiosity on the part of the authors to relate calm water predictions of wetted data to the dynamic wetted data in waves. The broken lines in Figure 15 to Figure 17 show the predicted wetted keel lengths from equation (7) with actual measured wetted keel lengths using CVDA. The results show very good agreement, as would be expected since the coefficients were varied until the predicted results match. However, Figure 21 shows the variation of the coefficients with wavelength and demonstrates a definite linear relationship for the coefficients with increasing wavelength. This implies that despite the simple approach outlined above, the calm-water time-independent wetted keel length predictions can be manipulated into evaluating the dynamic wetted keel length in waves. With this ability to predict the dynamic wetted lengths and given that the hydrodynamic forces are a function of wetted area, it would seem possible to evaluate dynamic lift and resistance given only limited data of beam and deadrise and the temporal data of heave and pitch.

It is important to note that the values for the fitted coefficients (A , B and C) and the assumed value for the mean wetted length of 3.75 in equation (7) will depend on many parameters. These values will change between different planing craft since they are intrinsic to each planing craft's design and operating and environmental conditions. The measurement of wetted chine lengths would no doubt significantly simplify the formulation of the above expressions.

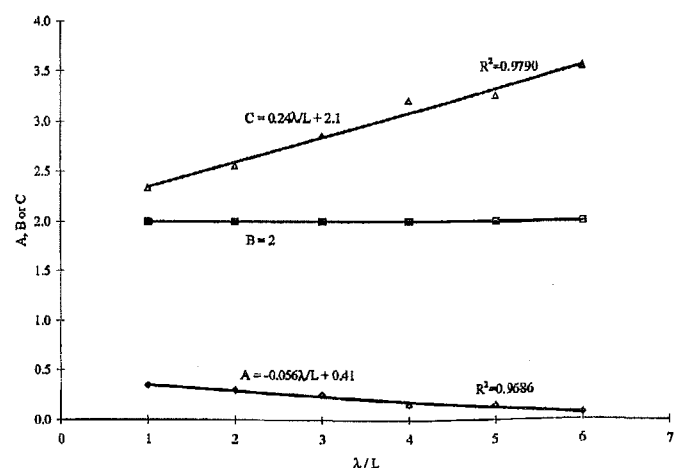


Figure 21 Behaviour of fitted coefficients (A , B and C) with wavelength

Troesch[21] employed a similar technique in investigating the dynamic variation of wetted lengths of craft undergoing forced perturbations in either heave or pitch. Equation (4) of that paper was plotted against Troesch's measured values from

analogue videotape analysis and showed excellent agreement between the predicted wetted keel lengths. Chine wetted lengths were not however as well predicted, but again correct identification of water/chine intersection was difficult due to the obtrusive presence of the spray jet.

3.3.2 Resistance In Waves

Savitsky's equations are based upon mean wetted lengths (an average of chine and keel wetted length) whereas the dynamic variation seems at first hand to be solely based on wetted keel lengths. However, the variation of the coefficients A , B and C allow for frequency dependence and chine wetted length variation – corrections for the assumption that L_c is not a function of time. Advancing the hypothesis that calm water equations may be applied in a dynamic sense using the aforementioned coefficients and temporal data for heave, pitch and wetted keel length, Savitsky's calm water equations for planing resistance are adapted.

From equation (1), calm water running trim angle, τ , is replaced by pitch angle $\theta(t)$. The lift coefficient, $C_{L0}(t)$, and skin friction coefficient, $C_f(t)$, are now also dependent on time and are defined assuming that the time-varying mean wetted length, $L_m(t)$, can be described by equation (6). From these assumptions, the results described in Figure 22 are produced and are compared to the authors' experimentally determined values. The values for mean resistance in waves are in fair agreement for all wavelenghts, especially if one considers the agreement between the predicted drag/lift ratio and the experimental drag/lift ratio described in Figure 12 for calm water performance. Savitsky's equation (equation (1)) over predicts the drag/lift ratio.

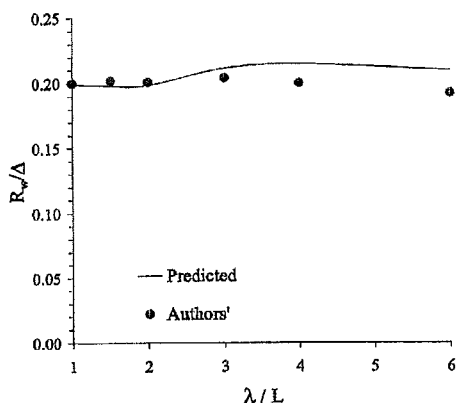


Figure 22 Comparison authors' experimental values for craft resistance in regular head seas and the resistance as predicted applying a quasi-steady variation to Savitsky's calm water equations.

4. CONCLUSIONS

Conducting planing craft experiments provides the necessary data by which to assess, validate and improve theory designed to predict and accurately simulate planing craft performance. However the dynamic phenomena associated with flow over planing hulls increases the complexity of accurately measuring the required quantities. Large scatter between the results of "identical" experimental programmes brings into question the validity of applying empirical fits for performance prediction. In order to help standardise the method by which planing craft experiments are practised, the CVDA system was initiated, tested and the results presented herein.

In Conclusion,

1. The use of a computer vision data acquisition technique demonstrated its importance in being able to identify specific points of interest and remotely capture large amounts of data.
2. The CVDA system was as successful in accurately acquiring motion data as the EDA approach.
3. In addition to the motion data, CVDA is able to measure the chine and keel wetted lengths. The wetted length values in calm water compared favourably with the results of 30 years previous[17].
4. The predictions of calm water wetted lengths from Savitsky's empirical calm water equations had favourable comparison with the values acquired through CVDA.
5. The ability of CVDA to measure the dynamic wetted keel lengths in waves resulted in the advancement of Savitsky's calm water equations to predict wetted keel lengths in waves. The inclusion of wetted chine length measurement using the CVDA approach should significantly improve the simplicity of the formulation.
6. The successful prediction of dynamic wetted lengths from calm water equations provided the encouragement to employ the same family of equations in a dynamic sense to quantify the lift forces and resistance in waves. The predicted results for craft resistance are favourable with experiments.

REFERENCES

- [1] Blake, J.I.R. 2000 Investigation into the vertical motions of high speed planing craft in calm water and in waves. PhD thesis. University of Southampton. May.
- [2] Payne, P. 1974 Coupled pitch and heave porpoising instability in hydrodynamic planing. *Ocean Engineering*, 8, 2, 58-71.
- [3] Payne, P. 1981 The vertical impact of a wedge on a fluid. *Ocean Engineering*, 8, 421-436.
- [4] Payne, P. 1982 The differences between a wing and a planing plate in two-dimensional flow. *Ocean Engineering*, 9, 5, 441-453.
- [5] Payne, P. 1984 On the high-speed porpoising instability of a prismatic hull. *Journal of Ship Research*, 28, 2, June, 77-89.
- [6] Payne, P. 1988 *Design of High Speed Boats – Planing*. 1 edition. Vol. 1. Fishergate, 2521 Riva Road, Annapolis, Maryland.
- [7] Payne, P. 1992 A unification in the added mass theory of planing. *Ocean Engineering*, 19, 1, 39-55.
- [8] Payne, P. 1993 The spray sheets produced during vertical wedge impact and steady planing. *Ocean Engineering*, 20, 3, 247-261.
- [9] Payne, P. 1994 Recent developments in 'added-mass' planing theory. *Ocean Engineering*, 21, 3, 257-309
- [10] Payne, P. 1995 Contributions to planing theory. *Ocean Engineering*, 22, 7, 699-729.
- [11] Sottorf, W. 1932 Experiments with planing surfaces. Technical Report. TM661. NACA.

- [12] Shoemaker, J. 1934 Tank tests of flat and vee-bottom planing surfaces. Technical Report. TN509. NACA. November
- [13] Sambras, A. 1938 Planing surface tests at large Froude numbers – airfoil comparison. Technical Report. TM1097. NACA. February.
- [14] Korvin-Kroukovsky, B., Savitsky, D., Lehman, W. 1949 Wetted area and centre of pressure of planing surfaces. Technical Report. 360 Stevens Institute of Technology. August.
- [15] Savitsky, D., Neldinger, J. 1954 Wetted area and centre of pressure of planing surfaces at very low speed coefficients. Technical Report. 493 Stevens Institute of Technology. July.
- [16] Savitsky, D. 1964 Hydrodynamic design of planing hulls. *Marine Technology*, October, 71-95.
- [17] Fridsma, G. 1969 A systematic study of the rough-water performance of planing boats. Technical Report. 1275. Stevens Institute of Technology. November.
- [18] Fridsma, G. 1971 A systematic study of the rough-water performance of planing boats (irregular waves – part ii). Technical Report. SIT-DL-71-1495. Stevens Institute of Technology. March.
- [19] Brown, P. 1971 An experimental and theoretical study of planing surfaces with trim flaps. Technical Report. R-47. Davidson Laboratory, Stevens Institute of Technology. November.
- [20] Koebel Jr., J.G., Stolz, J., Beinert, J.D. 1963 How to design planing hulls. Vol. 49, *Motor Boating*, Ideal Series.
- [21] Troesch, A. 1992 On the hydrodynamics of vertically oscillating planing hulls. *Journal of Ship Research*, December, 317-331

WRITTEN DISCUSSION

Dr Lewandowski: The Davidson Laboratory has been successfully determining wetted keel and chine length in calm water by use of underwater photographs for many years. The video system discussed in the paper would appear to be advantageous in that less setup effort is required; however, this might be at the expense of accuracy. The pressure area can be unmistakably identified in underwater photographs, whereas the spray root may well be obscured by the spray in above-water photos, particularly for lower deadrisers than the 30deg considered in the paper.

Note that there is a distinction between the pressure area, which is generally assumed to support the load, and the total wetted area, which includes the "spray area" forward of the spray root. As defined by Savitsky in Reference 16 of the paper, the wetted keel and chine lengths are to be measured from the spray root. However, the authors state that they were examining the "spray sheet/chine intersection" in their analysis of the video frames, which lies forward of the spray root line.

With regard to the comments relative to the "large amounts of instrumentation and equipment required to acquire all necessary data" in planing hull tests, the proposed methodology obviates the necessity for heave and trim/pitch transducers (and possibly accelerometers, although this remains to be demonstrated); these are minor contributors to the weight of the apparatus and calibration is straightforward. The drag transducer is typically the only instrument that contributes significantly to the weight of the model, and is required in both systems.

Would the authors care to comment on the lack of agreement of their measured trim with Fridsma's data (Figures 7 and 9)? This would indicate that the model and/or test conditions differed in the two tests, or that one of the data sets contains errors.

Finally, the point of the "wetted keel length" discussion is not clear. The utility of a formula such as Equation 7 is limited to cases in which one knows $L_m(t)$ as well as $z(t)$ and $\theta(t)$, but not $L_k(t)$. In practice one usually determines L_m from measurements of L_k and L_c . In addition, the form of Equation 7 does not appear to be correct, since the change in L_k resulting from vertical motion z should be inversely proportional to $\sin\theta$. We would propose a relationship of the form

$$L_k = A \left\{ x_0 + \frac{d_0 \cos \theta - z}{\sin \theta} \right\} + B$$

where x_0 and d_0 are the longitudinal and vertical coordinates of the towpoint (trim axis and heave reference point) relative to the transom and keel, respectively, and the heave z is to be measured from the calm water surface to the reference point (and thus is generally nonzero at zero speed), positive upwards. The quantity in brackets is the "static keel wetted length", which is the value one would obtain from geometry if there were no "dynamic wave rise".

Dr. Yukio Kaneko, (FRINA): I am a practical designer, neither an experimentalist nor a theorist. In my experience on several high-speed boats near planning or above, usually actual running trims are far less than calculated ones based on "Savitsky et al. s' methods". Many designers may have their own corrections on Prismatic Models. Even in case Prismatic Models, as authors of this paper point out, trimmings angles are scattered. There seems to be many reasons including experimental accuracies. In case of actual boats, running trim is preferable under 4°. If main reason exists on prismatic hull, experiments on modified prismatic hull should be carried out in future, for instance, horizontal part added to at chine line and its size varied systematically. If possible transverse, distribution of planing pressure will be useful.

AUTHORS REPLY:

The authors would like to thank **Dr Lewandowski** for his comments. The video system was driven by the need to capture information regarding wetted surface so as to enable validation and verification to be made to particular seakeeping characteristics predicted by a numerical model. Furthermore, the set-up was designed to be as simple as possible to enable the extension of monitoring wetted surface data on scale models to full scale testing. The authors recognise the importance of the work carried out by, amongst others, the Davidson Laboratory, and cite some of these works in the paper. Still photographs were considered to be an inappropriate method in obtaining transient data and so a video system was employed. It is true that the pressure area (of primary concern to a hydrodynamicist) can be most easily identified from under the water but measurement of vertical motions precluded this method. The chine wetted length was indeed measured by observation of the spray area, where the tail of the spray area intersecting with the chine was taken as the spray root line intersection with the chine.

Regarding the weight-saving in equipment, the authors acknowledge the relative contribution of each item of instrumentation to the total weight set aside for ballast and whilst any saving in weight is a bonus for high speed craft testing, the authors agree that the dynamometer contributes the largest proportion of the total weight and is necessary for resistance analyses by whichever method (either CVDA or EDA). However, the other benefits of CVDA in terms of cost, consistency of results and ease of setup remain.

an
be
ler
ide
obi

3.3

Sa
ave
van
lenq
allo
varl
fun
equ
afor
and
plan

Fr
by p
coef
defin
 $L_m(t)$
assu
and
value
agre
agre
expe
water
predi

R / A

Fig
craft
as pi
Savil

4. CC
Condu
data by
to predi
Howeve
planing l
the requ
"identica
validity c
order to
experime
tested ar

The discrepancies in trim and sinkage between Fridsma's results and the author's are quite large at higher speeds in calm water (leading to a subsequent change in regular wave performance). The reason for this is uncertain given that the craft in each case were tested under the "same" conditions - geometry, speed, mass distribution, etc. It may be seen to be too convenient to pass off the discrepancies as another example of the "problem of experimental repeatability" and make no further comment about this, but without further investigation into each test set-up we cannot determine the cause of the disagreements.

The discussion involving wetted keel length was driven by the observation that a simple measurement of wetted length could produce important information and good estimates on planing craft resistance. The formulation is not mathematically rigorously derived. The wetted keel length predicted in this manner was matched to the experimental results by assuming that the instantaneous value of wetted keel length was directly proportional to the craft's instantaneous trim angle - the effect of the inverse of the instantaneous trim angle in addition to the effect of trim. The coefficients employed in this highly empirical formulation were varied until the data matched experimental results. Using the contributor's more rigorously derived equation, the coefficients A and B are

found to have a similarly linear variation with respect to encounter frequency but the value of wetted keel length predicted in this manner is in less agreement with experimental measurements. Figure 23 shows the difference between wetted keel lengths predicted by the respective methods and the wetted keel length measured experimentally for wavelength/craft length of 3, 4 and 6. The extra coefficients in the author's formulation allow for a better fit to the data regardless of its scientific "correctness".

The authors would like to thank Dr Kaneko on his comments. The systematic study carried out by Fridsma was extremely important in quantifying the effects of changes to a prismatic planing hull. Further investigations were required in order to provide information on hull warping, stepped chines, spray rail placement and other features that pertain to more realistic sea-going designs. Experimental data from the systematic variation of such parameters is rare in the public domain. The authors agree that transverse pressure distributions would provide useful information on the fluid-structure interaction and be invaluable in the development of computational fluid dynamic solutions to the planing problem.

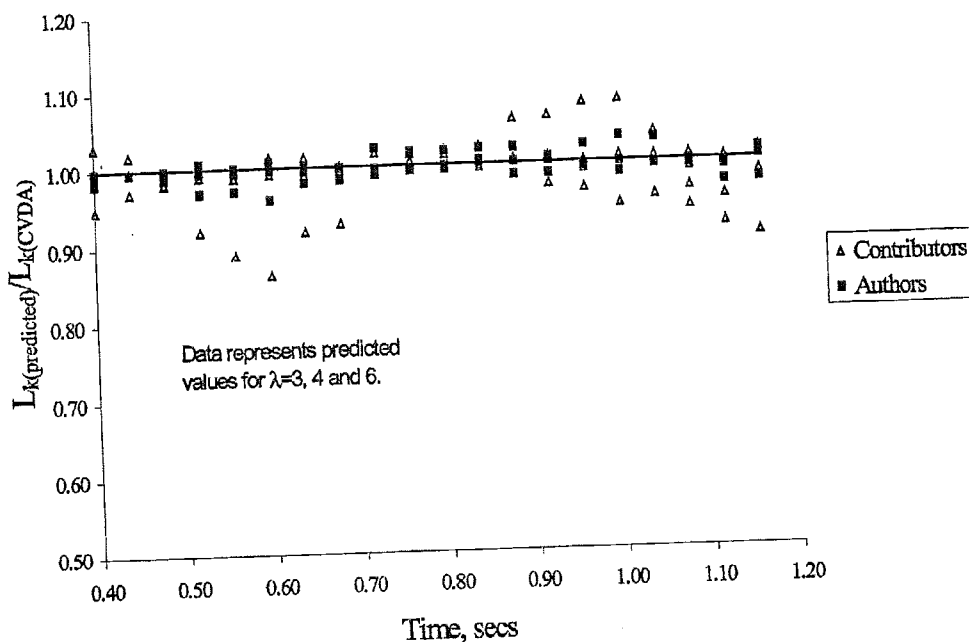


Figure 23. Error between the two prediction methods compared to the CVDA data for wetted keel length

